

HEAVY QUARK HADROPRODUCTION IN
 k_T -FACTORIZATION APPROACH WITH UNINTEGRATED
GLUON DISTRIBUTIONS

Yu.M.Shabelski and A.G.Shuvaev
Petersburg Nuclear Physics Institute,
Gatchina, St.Petersburg 188300 Russia

Abstract

We consider the processes of compare the heavy quark production using the unintegrated gluon distributions. The numerical predictions for high energy nucleon-nucleon and photon-nucleon collisions of the k_T -factorization approach (semihard theory) are compared with the experimental data from Tevatron-collider and HERA. The total production cross sections and p_T distributions are considered and they are in reasonable agreement with the data for rather value of QCD scale.

E-mail SHABELSK@THD.PNPI.SPB.RU

E-mail SHUVAEV@THD.PNPI.SPB.RU

1 Introduction

The investigation of heavy quark production in high energy hadron collisions is an important method for studying the quark-gluon structure of hadrons. The description of hard interactions in hadron collisions within the framework of QCD is possible only with the help of some phenomenology, which reduces the hadron-hadron interaction to the parton-parton one via the formalism of the hadron structure functions. The cross sections of hard processes in hadron-hadron interactions can be written as the convolutions squared matrix elements of the sub-process calculated within the framework of QCD, with the parton distributions in the colliding hadrons.

The most popular and technically simplest approach is the so-called QCD collinear approximation, or parton model (PM). In this model all particles involved are assumed to be on mass shell, carrying only longitudinal momenta, and the cross section is averaged over two transverse polarizations of the incident gluons. The virtualities q^2 of the initial partons are taken into account only through their structure functions. The cross sections of QCD sub-process are calculated usually in the next to leading order (NLO) of α_s series [1, 2, 3, 4]. The transverse momenta of the incident partons are neglected in the QCD matrix elements. This is the direct analogy of the Weizsaecker-Williams approximation in QED.

Another possibility to incorporate the incident parton transverse momenta is referred to as k_T -factorization approach [5, 6, 7, 8, 9, 10], or the theory of semihard interactions [11, 12, 13, 14, 15, 16, 17, 18, 19]. Here the Feynman diagrams are calculated taking account of the virtualities and of all possible polarizations of the incident partons. In the small x domain there are no grounds to neglect the transverse momenta of the gluons, q_{1T} and q_{2T} , in comparison with the quark mass and transverse momenta, p_{iT} . Moreover, at very high energies and very high p_{iT} the main contribution to the cross sections comes from the region of $q_{1T} \sim p_{1T}$ or $q_{2T} \sim p_{1T}$, see [20, 21, 22] for details. The QCD matrix elements of the sub-processes are rather complicated in such an approach. We have calculated them in the LO. On the other hand, the multiple emission of soft gluons is included here. That is why the question arises as to which approach is more constructive.

In Sect. 2 we present the cross sections of heavy quark production in hadron-nucleon and photon-nucleon collisions in the k_T -factorization approach. This approach accounts for the diagrams without neglecting by the virtualities of incident partons (mainly gluons), their polarization, etc. The detailed

discussion of the k_T -factorization approach, and its numerical difference from the parton model can be found in [21, 22].

The different approaches for the unintegrated gluon distributions are discussed in Sect. 3 and 4. We show that the difference between them is not very large, and after integration the unintegrated gluon distributions reproduce the initial structure functions. At the moment we have no more realistic unintegrated parton distributions which are extracted from the data by the same way as structure functions, i.e. by using the evolution equations, boundary conditions at some small Q_0^2 , etc.

The experimental data on heavy quark production at Tevatron-collider and HERA are discussed in Sect. 5. Our predictions with the selected k_T -factorization (which seems to be rather natural) are in reasonable agreement with p_T -distributions of b -quarks produced in FNAL, as well as with the data on total cross sections of charm and beauty production at HERA. Predictions of the k_T -factorization approach for heavy quark production at LHC are also given.

2 Heavy quark production in hadron-hadron and photon-hadron collisions in k_T -factorization approach

The conventional parton model expression for the calculation of heavy quark hadroproduction cross sections has the factorized form [23]:

$$\sigma(ab \rightarrow Q\bar{Q}) = \sum_{ij} \int dx_i dx_j g_{a/i}(x_i, \mu_F) g_{b/j}(x_j, \mu_F) \hat{\sigma}(ij \rightarrow Q\bar{Q}) , \quad (1)$$

where $g_{a/i}(x_i, \mu_F)$ and $g_{b/j}(x_j, \mu_F)$ are the structure functions of partons i and j in the colliding hadrons a and b , μ_F is the factorization scale (i.e. virtualities of incident partons) and $d\hat{\sigma}(ij \rightarrow Q\bar{Q})$ is the cross section of the direct subprocess ($ij \rightarrow \bar{Q}Q$ which is calculated in perturbative QCD. The last cross section can be written as a sum of LO and NLO contributions, and its analytical form can be found in [1, 2, 3, 4].

The principal problem of parton model is the collinear approximation. The transverse momenta of the incident partons, q_{iT} and q_{jT} are assumed to be zero, and their virtualities are accounted through the structure functions only; the

cross section $\hat{\sigma}(ij \rightarrow Q\bar{Q})$ is assumed to be independent on these virtualities. Naturally, this approximation essentially simplifies calculations.

Sometimes namely these simplifications result to the serious disagreement with the experimental data.

Without the discussed simplifications of PM, the differential cross section of heavy quark hadroproduction in LO QCD (Fig. 1) has the following form [11, 14]:¹

$$\begin{aligned} \frac{d\sigma_{pp}}{dy_1^* dy_2^* d^2 p_{1T} d^2 p_{2T}} &= \frac{1}{\pi^2} \frac{1}{(s')^2} \int d^2 q_{1T} d^2 q_{2T} \delta(q_{1T} + q_{2T} - p_{1T} - p_{2T}) \\ &\times \frac{\alpha_s(q_1^2)}{q_1^4} \frac{\alpha_s(q_2^2)}{q_2^4} f_g(y, q_{1T}, \mu) f_g(x, q_{2T}, \mu) |M_{QQ}|^2. \end{aligned} \quad (2)$$

Here we have used the Sudakov (light cone) decomposition for quark momenta $p_{1,2}$ through the momenta of colliding hadrons p_A and p_B ,

$$p_A^2 = p_B^2 \simeq 0, \quad 2p_A \cdot p_B = s', \quad (3)$$

and transverse ones $p_{1,2T}$:

$$p_{1,2} = x_{1,2} p_B + y_{1,2} p_A + p_{1,2T}. \quad (4)$$

In LLA kinematics

$$\begin{aligned} q_1 &\simeq y p_A + q_{1T}, & q_2 &\simeq x p_B + q_{2T}, \\ q_1^2 &\simeq -q_{1T}^2, & q_2^2 &\simeq -q_{2T}^2, \\ x &= x_1 + x_2, & y &= y_1 + y_2. \end{aligned} \quad (5)$$

(The more accurate relations are $q_1^2 = -q_{1T}^2/(1-y)$, $q_2^2 = -q_{2T}^2/(1-x)$ but we are working in the kinematics where $x, y \ll 1$).

$q_{1,2T}$ are the gluon transverse momenta;

$$\begin{aligned} x_1 &= \frac{m_{1T}}{\sqrt{s'}} e^{-y_1^*}, & y_1 &= \frac{m_{1T}}{\sqrt{s'}} e^{y_1^*}, \\ x_2 &= \frac{m_{2T}}{\sqrt{s'}} e^{-y_2^*}, & y_2 &= \frac{m_{2T}}{\sqrt{s'}} e^{y_2^*}, \\ m_{1,2T}^2 &= m^2 + p_{1,2T}^2, \end{aligned} \quad (6)$$

¹We put the argument of α_s to be equal to gluon virtuality, which is very close to the BLM scheme[24]; (see also [14]).

where $y_{1,2}^*$ are the quark rapidities in the hadron-hadron c.m.s. frame and m is the mass of produced heavy quark and we take these masses

$$m_c = 1.4 \text{ GeV} , m_b = 4.6 \text{ GeV} , \quad (7)$$

for the values of short-distance perturbative quark masses [25, 26]. $|M_{QQ}|^2$ is the square of the matrix element for the heavy quark pair hadroproduction. It is calculated in the Born approximation of QCD without standard simplifications of the parton model. Contrary to the mention of [18], the transformation Jacobian from x, y to y_1^*, y_2^* is accounted in our matrix element.

The unintegrated gluon distributions $f_g(y, q_{1T}, \mu)$ and $f_g(x, q_{2T}, \mu)$ will be discussed in details in the Sect. 3.

To provide the k_T factorization of eq.(2) the cross-section of the elementary subprocess for the heavy quarks production, $gg \rightarrow Q\bar{Q}$ was calculated in the axial gauge where the spin part of the gluon (q_i) propagator takes the form

$$d_{\mu\nu}(q_i) = g_{\mu\nu} - \frac{n_\mu q_{i,\nu} + q_{i,\mu} n_\nu}{(n \cdot q_i)}$$

with the gauge vector $n_\nu = (p_1 + p_2)_\nu - (p_1 + p_2)_{T,\nu}$ (that is $n_\nu = (n_0, 0, 0, 0)$ in the frame where the longitudinal part of quark pair momentum $(p_1 + p_2)_z = 0$).

In this gauge both the DGLAP and BFKL leading logarithms in the unintegrated distributions f_g are given by the ladder type diagrams shown in Fig.1 without any extra interactions between the upper and lower parts of the graphs (that is between the functions $f_g(x, q_{2T}, \mu)$ and $f_g(y, q_{1T}, \mu)$).

Being averaged over the colours of the incoming gluons the matrix element squared $|M_{QQ}|^2$ reads

$$\begin{aligned}
|M_{QQ}|^2 &= \frac{1}{x^2 y^2} \left\{ \frac{1}{4N_c} \left[\frac{m_{11}}{(m^2 - t)^2} + \frac{m_{22}}{(m^2 - u)^2} \right] \right. \\
&\quad - \frac{1}{4N_c} \frac{(m_{12} + m_{21})/2}{(m^2 - t)(m^2 - u)} \\
&\quad \left. + \frac{1}{2} N_c (N_c^2 - 1)^{-1} \frac{1}{s} \left[\frac{(m_{13} + m_{31})/2}{m^2 - t} - \frac{(m_{23} + m_{32})/2}{m^2 - u} + \frac{m_{33}}{s} \right] \right\}. \tag{8}
\end{aligned}$$

Here $N_c = 3$ is the number of colors, the variables s , t , u are defined for $gg \rightarrow Q\bar{Q}$ subprocess.

$$\begin{aligned}
m^2 - t &= m^2 + x_1 y_2 s' + (p_1 - q_1)_T^2 \\
m^2 - u &= m^2 + x_2 y_1 s' + (p_1 - q_2)_T^2 \\
s &= x y s' - (p_1 + p_2)_T^2
\end{aligned}$$

The elements m_{ik} are the numerators of the lowest order QCD Born diagrams squared and averaged over quark helicities; the incoming transverse momenta $q_{1,2T}$ play the role of gluon polarization vectors,

$$\begin{aligned}
m_{11} &= \text{Sp} (\hat{p}_1 + m) \hat{q}_{1T} (\hat{p}_1 - \hat{q}_1 + m) \hat{q}_{2T} (\hat{p}_2 - m) \hat{q}_{2T} (\hat{p}_1 - \hat{q}_1 + m) \hat{q}_{1T} \\
m_{21} &= \text{Sp} (\hat{p}_1 + m) \hat{q}_{1T} (\hat{p}_1 - \hat{q}_1 + m) \hat{q}_{2T} (\hat{p}_2 - m) \hat{q}_{1T} (\hat{p}_1 - \hat{q}_2 + m) \hat{q}_{2T} \\
m_{22} &= \text{Sp} (\hat{p}_1 + m) \hat{q}_{2T} (\hat{p}_1 - \hat{q}_2 + m) \hat{q}_{1T} (\hat{p}_2 - m) \hat{q}_{1T} (\hat{p}_1 - \hat{q}_2 + m) \hat{q}_{2T} \\
m_{31} &= \text{Sp} (\hat{p}_1 + m) \hat{V}_3 (\hat{p}_2 - m) \hat{q}_{2T} (\hat{p}_1 - \hat{q}_1 + m) \hat{q}_{1T} \\
m_{32} &= \text{Sp} (\hat{p}_1 + m) \hat{V}_3 (\hat{p}_2 - m) \hat{q}_{2T} (\hat{p}_1 - \hat{q}_2 + m) \hat{q}_{2T} \\
m_{33} &= \text{Sp} (\hat{p}_1 + m) \hat{V}_3 (\hat{p}_2 - m) \hat{V}_3,
\end{aligned}$$

$$m_{12} = m_{21}, \quad m_{13} = m_{31}, \quad m_{23} = m_{32}.$$

The matrix

$$\hat{V}_3 = q_{1T} \cdot q_{2T} (\hat{q}_1 - \hat{q}_2) - ((2q_1 + q_2) \cdot q_{2T}) \hat{q}_{1T} + ((2q_2 + q_1) \cdot q_{1T}) \hat{q}_{2T}$$

is the contribution of a triple gluon vertex.

Thus we can calculate the heavy quark production cross section without standart simplifications of the parton model since in the small x region there are no grounds for neglecting the transverse momenta of the gluons $q_{1,2T}$ in comparison with the quark mass and transverse momenta $p_{1,2T}$. Although

explicit expressions for m_{ik} are rather bulky, they can be easily computed using any analytical computer program (say, REDUCE or MATHEMATICA). For example, the dependence of the matrix elements on the gluon transverse momenta is a main source for the nontrivial azimuthal correlations arising between quarks momenta $p_{1,2T}$ which could not be described in the conventional parton model.

In the case of high energy heavy quark photoproduction on the proton target we should consider two possibilities, the same resolved production via quark-gluon structure of the photon, Fig. 1, where one proton should be replaced by photon (with its parton distribution, different from the case of incident nucleon), and direct production in the photon-gluon fusion, $\gamma p \rightarrow Q\bar{Q}$, Fig. 2, where the incident photon has the fixed momentum.

The cross section of the direct interaction can be written by the same way as Eq. (2) where the unintegrated gluon distribution $f_g(y, q_{1T}, \mu)$ should be replaced by $\delta(y-1)$. The cross section of the direct interaction can be written as

$$\frac{d\sigma_{\gamma p}}{d^2p_{1T}} = \frac{\alpha_{em}e_Q^2}{\pi} \int dz d^2q_T \frac{f_g(x, q_T, \mu)}{q_T^4} \alpha_s(q^2) \times \left\{ [(1-z)^2 + z^2] \left(\frac{\vec{p}_{1T}}{D_1} + \frac{\vec{q}_T - \vec{p}_{1T}}{D_2} \right)^2 + m_Q^2 \left(\frac{1}{D_1} - \frac{1}{D_2} \right)^2 \right\}, \quad (9)$$

$$D_1 = p_{1T}^2 + m_Q^2, \quad D_2 = (\vec{q}_T - \vec{p}_{1T})^2 + m_Q^2, \quad (10)$$

here $\alpha_{em} = 1/137$ and e_Q is the electric charge of the produced heavy quark.

3 Unintegrated gluon distributions in different approaches

The unintegrated parton distribution $f_a(x, q_T, \mu)$ determines the probability to find a parton a initiating the hard process with the transverse momentum q_T (and with factorization scale μ).

At very low x , that is to leading $\log(1/x)$ accuracy, for the case of q_T of the order of scale μ the unintegrating gluon distribution are approximately determined [11] via the derivative of the usual structure function:

$$f_g(x, q_T, \mu) \simeq f_g(x, q^2) = \frac{\partial[xg(x, q^2)]}{\partial \ln q^2}. \quad (11)$$

However at a large x the unintegrated density (11) becomes negative.

To restore the function $f_a(x, q_T, \mu)$ on the basis of the conventional (integrated) parton density $a(x, \lambda^2)$ we have to consider the DGLAP evolution²

$$\frac{\partial a}{\partial \ln \lambda^2} = \frac{\alpha_s}{2\pi} \left[\int_x^\Delta P_{aa'}(z) a'\left(\frac{x}{z}, \lambda^2\right) dz - a(x, \lambda^2) \sum_{a'} \int_0^\Delta P_{a'a}(z') dz' \right]. \quad (12)$$

Here, $a(x, q_1^2)$ denotes $xg(x, q_1^2)$ or $xq(x, q_1^2)$, and $P_{aa'}$ are the splitting functions.

The first term on the right-hand side of Eq. (12) describes the number of partons δ_a emitted in the interval $\lambda^2 < q_T^2 < \lambda^2 + \delta\lambda^2$, while the second (virtual) term reflects the fact that the parton a disappears after the splitting.

The second contribution may be resummed to give the survival probability T_g that gluon g with the transverse momentum q_T remains untouched in the evolution up to the factorization scale

$$T_g(q_T, \mu) = \exp \left[- \int_{q_T^2}^{\mu^2} \frac{\alpha_s(p_T)}{2\pi} \frac{dp_T^2}{p_T^2} \sum_{a'} \int_0^\Delta P_{a'g}(z') dz' \right]. \quad (13)$$

Thus, the unintegrated gluon distribution $f_g(x, q_T, \mu)$ has the form

$$f_g(x, q_T, \mu) = \sum_{a'} \left[\frac{\alpha_s}{2\pi} \int_x^\Delta P_{ga'}(z) a'\left(\frac{x}{z}, q_T^2\right) dz \right] T_g(q_T, \mu), \quad (14)$$

where the cut-off Δ is used in Eqs. (12-14) [30, 31].

The expression (14) with the survival probability (13) provides the positivity of the unintegrated probability $f_g(x, q_T, \mu)$ in the whole interval $0 < x < 1$. It is necessary to note that the calculation of the integrals in Eqs. (13) and (14) should be fulfilled with rather high and equal accuracy because the factor $T_g(q_T, \mu)$ compensate the singularity at $\Delta \rightarrow 1$ in Eq. (14).

For the case of one loop QCD running coupling $\alpha_s(p_T) = 4\pi/(b \ln p_T^2/\Lambda^2)$ the factor $T_a(q_T, \mu)$ can be written down explicitly. In particular, the gluon survival probability (which enters our formulae) reads:

$$T_a(q_T, \mu) = \frac{\ln(\mu/\Lambda)}{\ln(q_T/\Lambda)} \cdot \exp \left\{ \frac{8N_c}{b} \left[\ln \frac{\mu}{q_T} - \ln \frac{\mu}{\Lambda} \ln \frac{\ln(\mu/\Lambda)}{\ln(q_T/\Lambda)} - 2E_1(q_T, \mu) + 3/2 E_2(q_T, \mu) - \right. \right.$$

²For the $g \rightarrow gg$ splitting we need to insert a factor z' in the last integral of Eq. (12) to account for the identity of the produced gluons.

$$-2/3E_3(q_T, \mu) + 1/4E_4(q_T, \mu)] + \quad (15)$$

$$+ \frac{2}{3b} n_F [3E_1(q_T, \mu) - 3E_2(q_T, \mu) + 2E_3(q_T, \mu)] \}$$

where

$$E_k(q_T, \mu) = \left(\frac{\Lambda}{\mu} \right)^k [Ei(k \ln(\mu/\Lambda)) - Ei(k \ln(q_T/\Lambda))] , \quad (16)$$

and the integral exponent $Ei(z) = \int_{-\infty}^z \frac{dt}{t} \exp t$; n_F and N_c are the number of light quark flavours and the number of colours, respectively, and $b = 11 - \frac{2}{3}n_F$.

In the leading $\log(1/x)$ (i.e. BFKL) limit the virtual DGLAP contribution is neglected. The scale μ is of the order of q_T . So $T_a = 1$ and one comes back to Eq. (11)

$$f_a^{BFKL}(x, q_T, \mu) = \frac{\partial a(x, \lambda^2)}{\partial \ln \lambda^2} , \lambda = q_T . \quad (17)$$

In the double log limit Eq. (12) can be written in the form

$$f_a^{DDT}(x, q_T, \mu) = \frac{\partial}{\partial \ln \lambda^2} [a(x, \lambda^2) T_a(\lambda, \mu)]_{\lambda=q_T} , \quad (18)$$

which was firstly proposed by [30]. In this limit the derivative $\partial T_a / \partial \ln \lambda^2$ cancels the second term of the r.h.s. of Eq. (12) (see [31] for a more detailed discussion)³.

Finally, the probability $f_a(x, q_T, \mu)$ is related to the BFKL function $\varphi(x, q_T^2)$ by

$$\varphi(x, q_T^2) = 4\sqrt{2} \pi^3 f_a(x, q_T, \mu) / q_T^2 . \quad (19)$$

Note that due to a virtual DGLAP contribution the derivative $\partial a(x, \lambda^2) / \partial \lambda^2$ can be negative for not small enough x values. This shortcoming of Eq. (17) is partly overcome in the case of Eq. (18).

We have to emphasize that $f_g(x, q_T, \mu)$ is just the quantity which enters into the Feynman diagrams. The distributions $f_g(x, q_T, \mu)$ involve two hard

³There is a cancellation between the real and virtual soft gluon DL contributions in the DGLAP equation, written for the integrated partons (including all $k_T \leq \mu$). The emission of a soft gluon with momentum fraction $(1-z) \rightarrow 0$ does not affect the x -distribution of parent partons. Thus the virtual and real contributions originated from $1/(1-z)$ singularity of the splitting function $P(z)$ cancel each other. On the contrary, in the unintegrated case the emission of soft gluon (with $q'_T > k_T$) alters the transverse momentum of parent (t -channel) parton.

scales⁴: q_T and the scale μ of the probe. The scale μ plays a dual role. On the one hand it acts as the factorization scale, while on the other hand it controls the angular ordering of the partons emitted in the evolution [32, 33, 34]. The factorization scale μ separates the partons associated with the emission off both the beam and target protons (in pp collisions) and off the hard subprocess. For example, it separates emissions off the beam (with polar angle $\theta < 90^\circ$ in c.s.m.) from those off the target (with $\theta > 90^\circ$ in c.s.m.), and from the intermediate partons from the hard subprocess. This separation was proved in [32, 33, 34] and originates from the destructive interference of the different emission amplitudes (Feynman diagrams) in the angular boundary regions.

If the longitudinal momentum fraction is fixed by the hard subprocess, then the limits of the angles can be expressed in terms of the factorization scale μ which corresponds to the upper limit of the allowed value of the s -channel parton k_T .

4 Numerical values of unintegrated gluon distributions

As was shown above, there exist several ways for estimation the gluon unintegrated distributions. Now we will compare numerically several of them to see the theoretical uncertainties which should result in the uncertainties in the predictions for cross sections of heavy quark production.

First of all, it is evident that unintegrated gluon distributions obtained with the help of Eqs. (12)-(14) should coincide after their integration over q^2 with the used structure functions,

$$xg(x, q^2) = \int \frac{dq^2}{q^2} f_g(x, q_T, \mu) . \quad (20)$$

Some problem is that the values of $f_g(x, q_t, \mu)$ are principally unknown at very small $q_T^2 \simeq q^2$. So instead of Eq. (20) we can write

$$xg(x, q^2) = xg(x, q_0^2) + \int_{q_0^2} \frac{dq^2}{q^2} f_g(x, q_T, \mu) . \quad (21)$$

⁴This property is hidden in the conventional parton distributions as q_T is integrated up to the scale μ .

with $q_0^2 \sim 1 \text{ GeV}^2$.

The calculated values of heavy quark production cross sections depend [36] on the analytical form of the cut-off parameter Δ in Eqs. (12)-(14). However, if Eqs. (13) and (14) are calculated with the same numerical accuracy, this dependence becomes rather weak.

Now we compare the results for sum rules, Eq. (21), for two cases,

$$\Delta = \frac{\mu}{\mu + q_T} \quad (22)$$

and

$$\Delta = \frac{\mu}{\sqrt{\mu^2 + q_T^2}}. \quad (23)$$

The results of calculations are presented in Fig. 3a and one can see that the variants (22) and (23) give practically the same results. In the further numerical calculations we will use the variant (22) which corresponds to the angular ordering in the gluon emission [32, 33, 35].

In Fig. 3b we compare the q^2 dependences of unintegrated gluon distributions given by Eq.(14) [31], the KMS distribution [37], which was based on the BFKL equation and fitted to the F_2 HERA data just in unintegrated form, and simplified formula (11) [11]. In the first case we present the results for the value of QCD scale μ^2 in Eqs. (13), (14) equal to 100 GeV^2 (i.e. about $4m_b^2$). Here we have used rather more or less realistic gluon distribution GRV94 HO [38] which is compatible with the most recent data, see discussion in Ref. [39]. For a low x all three distributions are rather close to each other while at a larger $x \sim 0.05$ the KMR prescription gives for $q^2 > 10 \text{ GeV}^2$ about twice larger gluon density.

Eq. (2) enables us to calculate straightforwardly all distributions concerning one-particle or pair production. One-particle calculations as well as correlations between two produced heavy quarks can be easily done using, say, the VEGAS code [40].

However there exists a principle problem coming from the infrared region. Since the functions $\varphi(x, q_i^2)$ as well as $f_g(x, q_{Ti}^2, \mu)$ are unknown at small values of q_2^2 and q_1^2 , i.e. in nonperturbative domain we calculate separately the contributions from $q_1^2 < Q_0^2$, $q_2^2 < Q_0^2$, $q_1^2 > Q_0^2$ and $q_1^2 > Q_0^2$ [20, 21, 22].

$$\begin{aligned}
& \int d^2 q_{1T} d^2 q_{2T} \delta(q_{1T} + q_{2T} - p_{1T} - p_{2T}) \frac{\alpha_s(q_1^2)}{q_1^4} \frac{\alpha_s(q_2^2)}{q_2^4} f_g(y, q_{1T}, \mu) f_g(x, q_{2T}, \mu) |M_{QQ}|^2 = \\
& = \alpha_s^2(Q_0^2) x g(x, Q_0^2) y g(y, Q_0^2) T^2(Q_0^2, \mu^2) \left(\frac{|M_{QQ}|^2}{q_1^2 q_2^2} \right)_{q_{1,2} \rightarrow 0} + \quad (24) \\
& + \alpha_s(Q_0^2) x g(x, Q_0^2) T(Q_0^2, \mu^2) \int_{Q_0^2}^{\infty} dq_{1T}^2 \delta(q_{1T} - p_{1T} - p_{2T}) \times \\
& \quad \times \frac{\alpha_s(q_1^2)}{q_1^4} f_g(y, q_{1T}, \mu) \left(\frac{|M_{QQ}|^2}{q_2^2} \right)_{q_2 \rightarrow 0} + \\
& + \alpha_s(Q_0^2) y g(y, Q_0^2) T(Q_0^2, \mu^2) \int_{Q_0^2}^{\infty} dq_{2T}^2 \delta(q_{2T} - p_{1T} - p_{2T}) \times \\
& \quad \times \frac{\alpha_s(q_2^2)}{q_2^4} f_g(x, q_{2T}, \mu) \left(\frac{|M_{QQ}|^2}{q_1^2} \right)_{q_1 \rightarrow 0} + \\
& + \int_{Q_0^2}^{\infty} d^2 q_{1T} \int_{Q_0^2}^{\infty} d^2 q_{2T} \delta(q_{1T} + q_{2T} - p_{1T} - p_{2T}) \times \\
& \quad \times \frac{\alpha_s(q_1^2)}{q_1^4} \frac{\alpha_s(q_2^2)}{q_2^4} f_g(y, q_{1T}, \mu) f_g(x, q_{2T}, \mu) |M_{QQ}|^2,
\end{aligned}$$

where the unintegrated gluon distributions $f_g(x, q_T, \mu)$ are taken from Eq. (14). In the numerical calculations we use the values $\mu^2 = m_T^2$, $\mu^2 = 4m_T^2$ and $\mu^2 = \hat{s}$.

The first contribution in Eq. (24) ($q_1^2 < Q_0^2$, $q_2^2 < Q_0^2$) with the matrix element averaged over directions of the two-dimensional vectors q_{1T} and q_{2T} is exactly the same as the conventional LO parton model expression. It is multiplied by the 'survival' probability $T^2(Q_0^2, \mu^2)$ not to have transverse momenta $q_{1T}, q_{2T} > Q_0$. We assume $Q_0^2 = 1 \text{ GeV}^2$. The sum of the produced heavy quark momenta is taken to be exactly zero here.

The next three terms (when one, or both $q_{Ti}^2 > Q_0^2$) contain the corrections to the parton model due to account the different gluon polarizations, their virtualities and transverse momenta in the matrix element. The relative contribution of these corrections strongly depends on the initial energy. If it is not high enough, the first term dominates, and all results are similar to the conventional LO parton model predictions [21]. In the case of very high energy the opposite situation takes place, the first term can be considered as a small correction and our results differ from the conventional ones. So we need the highest energies for investigation the k_T -factorization effects.

5 Heavy quark production in the k_T -factorization approach

Let us compare the results of our numerical calculations with the data on beauty production at Tevatron-collider. In Fig. 4a we present the data [41] on b quark production with $p_T > p_{min}$ identified by its muon decay, as the function of p_{min} at 1.8 TeV. The curves of different type show the calculated results with different scales μ^2 in (13) and (14), $\mu^2 = m_T^2$, $\mu^2 = 4m_T^2$ and $\mu^2 = \hat{s}$, respectively, where \hat{s} is the invariant energy of the produced heavy quark pair, $\hat{s} = xys$. The calculated values of one-particle E_T distributions, $d\sigma/dE_T$, in k_T -factorization approach are presented in Fig. 4b together with the data [42] extracted from muon tagged jets. In both Figs. 4a and 4b our results are slightly smaller than the data.

The similar data on $b\bar{b}$ production with $p_T > p_{min}$ obtained by UA1 (circles) and CDF Coll. (Triangle point) at $\sqrt{s} = 630$ GeV taken from [43] are presented in Fig. 4c together with the results of our calculations. Again, our results are in agreement with UA1 and slightly smaller than the CDF data. Some disagreement between UA1 and CDF experimental data is evident.

The experimental data for charm production [44] at 1.96 TeV are compared with our calculations in Fig. 5. Now our curves slightly overestimate the data.

Table 1 The total cross sections of charm and beauty production in the k_T -factorization approach for $\mu^2 = m_Q^2$.

	all rapidities		$ y_Q < 1$	
\sqrt{s}	$c\bar{c}$	$b\bar{b}$	$c\bar{c}$	$b\bar{b}$
14 TeV	18.8 mb	0.92 mb	4.24 mb	0.245 mb
1.96 TeV	2.95 mb	89.6 μ b	843 μ b	33.3 μ b
1.8 TeV	2.7 mb	84.5 μ b	780 μ b	30.2 μ b

The energy dependences of the total cross sections of $c\bar{c}$ and $b\bar{b}$ pair production are presented in Table 1.

As it was mentioned, at comparatively small energies the first term in Eq. (24) dominates and the result of k_T -factorization approach practically coincides with LO parton model prediction. With increasing of the energy the

difference between the considered approaches increases and at the LHC energy the k_T -factorization predictions are about two times larger than the LO parton model ones (i.e. of the order of NLO parton model predictions). Generally, the k_T -factorization yields a more strong energy dependences both for $c\bar{c}$ and $b\bar{b}$ production. It can be explained by additional contributions appearing at very high energies in the k_T -factorization approach, see [20]. The main part of these contributions corresponds to the configurations where the transverse momentum of heavy quark is balanced not by another heavy quark but by the q_T of gluons.

Note that we underestimate the b -quark cross section but overestimate the charm production. This may be caused either by the behaviour of the gluon densities used in the calculations (too low density in the kinematical region ($x \sim 0.01$, $\mu^2 \sim 50 \text{ GeV}^2$) corresponding to the beauty production at the Tevatron and too high density at a lower scale and x relevant for the charm production) or this may indicate some experimental problem in selecting the b -quark events. Not excluded that sometimes the muon or jet from a charm production (which has a much larger cross section) was treated as the lepton/jet coming from the beauty.

It is not quite clear what the renormalization scale μ_R should be used as the argument of QCD coupling α_s in Eqs. (2) and (24) within the LO approximation of k_T -factorization approach. As the main version in the present paper we choose $\mu_R = Q_i^2$, motivated by BLM prescription [24]. On the other hand, based on the explicit one-loop calculation in Ref. [30], the argument was given in favour of the running coupling depending on the largest virtuality in the ladder cell under consideration⁵.

By this reason in Fig. 4a we present the curve corresponding to the $\mu_R = m_T$ (that is in Eq. (24) we put the coupling $\alpha_s(m_T)$). For the case of beauty production this choice reduces the predicted cross section of about $2 \div 3$ times for $p_{Tmin} = 5\text{--}30 \text{ GeV}/c$, respectively. However for a lighter charm quark using the $\alpha_s(m_T)$ we obtain the cross section only $1.2 \div 1.5$ times smaller than that with $\alpha_s(q_i^2)$.

Heavy quark production at the Tevatron within the framework of k_T -factorization was studied recently in [45]. The authors used the unintegrated gluon densities obtained from the Linked Dipole Chain model. With the "standard" gluons they obtained the results close to our calculations and underesti-

⁵The preexponent factor $\ln(\mu/\Lambda)/\ln(q_T/\Lambda)$ in Eq. (15) effectively replaces the one-loop running coupling $\alpha_s(\mu)$ by the $\alpha_s(q_T)$, close to the BLM prescription [24].

mated the beauty cross section extracted from the measurement of the muon and jet distributions. To describe the data it was needed to take so-called "leading" gluons, that is the version of the model which neglects the light quark contribution and the non-singular terms in the splitting functions. We see no possibility to justify such an approach.

On the other hand the new CDF data where the B -meson was identified via the $B \rightarrow J/\Psi X$ decay mode give a lower cross section. The last analysis of this new CDF data gives $29.4_{-5.4}^{+6.2} \mu\text{b}$ [46] in agreement with our result ($25 \mu\text{b}$) for beauty production at 1.96 TeV for $|y_b| < 1$.

The energy dependences of the total cross sections of $c\bar{c}$ and $b\bar{b}$ photoproduction are presented in Fig. 6. The data on charm (Fig. 6a) and beauty (Fig. 6b) photoproduction cross sections are taken from [47, 48, 49]. All three values, used for the scale give very similar results which are again slightly lower than the high energy data. Here we show separately the sum of direct and resolved contributions, as well as the only resolved ones. The resolved contributions have more strong energy dependence. At energies $W \sim 300$ GeV they give 12 – 15% of the total cross sections but in some kinematical regions they can even dominate [36], for example, in the target fragmentation region. The resolved contributions decrease with p_T more fast, that is connected with the finite phase space value.

6 Conclusion

We have compared the k_T -factorization approach for heavy quark hadro- and photoproduction at collider energies with the existing experimental data. The agreement is reasonable when we use the cut-off (22) in Eqs. (13) and (14) and it does not practically depends on the value of QCD scale μ in these equations. We present also some predictions for the total cross sections of heavy quark production at LHC energies.

Another example of very successful comparison of experimental data with the k_T -factorization approach can be found in [10] where some different assumptions were used.

It has been shown in Sect. 4 of [20] that the contribution of the domain with strong q_T ordering ($q_{1T}, q_{2T} \ll m_T = \sqrt{m_Q^2 + p_T^2}$) coincides in the k_T -factorization approach with the LO PM prediction. Besides this a numerically large contribution appears at high energies in k_T -factorization approach in

the region $q_{1,2T} \geq m_T$. This kinematically relates to the events where the transverse momentum of heavy quark Q is balanced not by the momentum of antiquark \bar{Q} but by the momentum of the nearest gluon.

An interesting consequence of such a kinematics is the fact that even at large transverse momentum $p_{1T} \gg m$ the ratio of the single quark inclusive cross sections for charm and beauty production $R_{c/b} = (d\sigma_c/d^3p)/(d\sigma_b/d^3p)$ does not tend to unity. At Tevatron-LHC energies this ratio $R_{c/b} \simeq 1.5$ and only selecting the events where both quarks has a large p_T we obtain the ratio close to unit (the difference $R_{c/b} - 1$ does not exceed a few per cents when both $p_{1T}, p_{2T} > 40$ GeV).

The configurations with $q_{1,2T} \geq m_T$ are associated with the NLO (or even NNLO, if both $q_{1T}, q_{2T} \geq m_T$) corrections in terms of the PM with fixed number of flavours, i.e. without the heavy quarks in the evolution. Indeed, as was mentioned in [1], up to 80% of the whole NLO cross section originates from the events where the heavy quark transverse momentum is balanced by the nearest gluon jet. Thus the large "NLO" contribution, especially at large p_T , is explained by the fact that the virtuality of the t -channel (or u -channel) quark becomes small in the region $q_T \simeq p_T$, and the singularity of the quark propagator $1/(\hat{p} - \hat{q} - m_Q)$ in the "hard" QCD matrix element, $M(q_{1T}, q_{2T}, p_{1T}, p_{2T})$, reveals itself.

The double logarithmic Sudakov-type form factor T in the definition of the unintegrated parton density Eq. (14) comprises an important part of the virtual loop NLO (with respect to the PM) corrections. Thus we demonstrate that the k_T -factorization approach collects already at the LO the major part of the contributions which play the role of the NLO (and even NNLO) corrections to the conventional PM. Therefore we hope that a higher order (in α_S) correction to the k_T -factorization could be rather small.

Recall that our results are rather stable with respect of the factorization scale μ variations and with respect to the form of angular cut-off parameter Δ in (22, (23).

Another advantage of this approach is that a non-zero transverse momentum of $Q\bar{Q}$ -system ($p_{T_{pair}} = p_{1T} + p_{2T} = q_{1T} + q_{2T}$) is naturally achieved in the k_T -factorization. We have calculated in [21, 22] the $p_{T_{pair}}$ distribution and compared it with the single quark p_T spectrum. At the low energies the typical values of $p_{T_{pair}}$ are much lesser than the heavy quark p_T in accordance with collinear approximation. However for LHC energy both spectra become close to each other indicating that the transverse momentum of second heavy

quark is relatively small. The typical value of this momentum depends on the parton structure functions/densities. It increases with the initial energy and with the transverse momenta of the heavy quarks, p_T . Thus one gets a possibility to describe a non-trivial azimuthal correlation without introducing a large "phenomenological" intrinsic transverse momentum of the partons.

The contribution coming from $q_T > \mu$ region could enhance the flux of colliding gluons and by this way partly explain the FNAL-Tevatron puzzle – data on the cross section of $b\bar{b}$ (or high- p_T prompt photon) production are 2-3 times larger than the conventional NLO PM QCD predictions [31, 41, 50]⁶.

At the moment we have no realistic unintegrated parton distributions which fit the data with accounting for the contribution from $q_T > \mu$. We hope that future experiments will allow to distinct between different approaches. It is necessary to note is that the theoretical results concern the heavy quarks rather than the hadron production which can be investigated experimentally. The hadronization leads to several important effects, however their description needs additional phenomenological assumptions, see e.g. [51, 52, 53].

We are grateful to M.G.Ryskin for many useful discussions. This paper was supported in part by grants RCGSS-1124.2003.2 and NATO PDD (CP) PST.CLG 980287.

⁶Recall, however, that the analysis [46] of the new CDF data gives a lower beauty production cross section.

Figure Captions

Fig. 1. Low order QCD diagrams for heavy quark production in pp ($p\bar{p}$) collisions via gluon-gluon fusion.

Fig. 2. Low order QCD diagrams for heavy quark production in direct γp collisions via photon-gluon fusion.

Fig. 3. The unintegrated gluon distributions integrated over q_T^2 until $Q^2 = 100 \text{ GeV}^2$ using Eq. (21) for $\Delta = \mu/(\mu + q_T)$ (dashed curve) and $\Delta = \mu/\sqrt{\mu^2 + q_T^2}$ (dotted curve) with $\mu^2 = Q^2$ together with gluon structure function GRV94 HO (solid curve) which was used for the calculations of these unintegrated distributions using Eq. (14) (a). The comparison of KMR, Eq. (14) (solid curves), GLR, Eq. (11) (dotted curves) and KMS [37] (dash-dotted curves) unintegrated gluon distributions at $x = 0.0005$ (upper curves) and $x = 0.05$ (lower curves) (b).

Fig. 4. The cross sections for beauty production for p_T higher than p_T^{min} (a, c) and $d\sigma/dE_T$ (b) in $p\bar{p}$ collisions at 1.8 TeV (a,b) with $|y_1| < 1$, and 0.63 TeV $|y_1| < 1.5$, (c) and their description by the k_T -factorization approach with unintegrated gluon distribution $f_g(x, q_T, \mu)$ given by Eq. (14). The value of Δ in Eq. (13), (14) was taken equal to $\mu/(q_T + \mu)$ with the scale values $\mu^2 = m_T^2$ (solid curves, $\mu^2 = 4m_T^2$ (dashed curves) and $\mu^2 = \hat{s}$ (dotted curves).

Fig. 5. The cross sections for charm production in $p\bar{p}$ collisions at 1.96 TeV with $|y_1| < 1$ and their description by the k_T -factorization approach with unintegrated gluon distribution $f_g(x, q_T, \mu)$ given by Eq. (14). The value of Δ in Eq. (13), (14) was taken equal to $\mu/(q_T + \mu)$ with the scale values $\mu^2 = m_T^2$ (solid curves, $\mu^2 = 4m_T^2$ (dashed curves) and $\mu^2 = \hat{s}$ (dotted curves).

Fig. 6. Total cross sections of charm (a) and beauty (b) photoproduction. The values of Δ in Eq. (13), (14) were taken equal to $\mu/(q_T + \mu)$ with scale values $\mu^2 = m_T^2$ (solid curves), $\mu^2 = 4m_T^2$ (dotted curves) and $\mu^2 = \hat{s}$ (dashed curves). The resolved photon contributions are shown by lower solid curves.

References

- [1] P.Nason, S.Dawson and R.K.Ellis. Nucl.Phys. B303 (1988) 607.
- [2] P.Nason, S.Dawson and R.K.Ellis. Nucl.Phys. B327 (1989) 49.
- [3] W.Beenakker, H.Kuijf, W.L.Van Neerven and J.Smith. Phys.Rev. D40 (1989) 54.
- [4] W.Beenakker, W.L.Van Neerven, R.Meng, G.A.Schuler and J.Smith. Nucl.Phys. B351 (1991) 507.
- [5] S.Catani, M.Ciafaloni and F.Hautmann. Phys.Lett. B242 (1990) 97; Nucl.Phys. B366 (1991) 135.
- [6] J.C.Collins and R.K.Ellis. Nucl.Phys. B360 (1991) 3.
- [7] G.Marchesini and B.R.Webber. Nucl.Phys. B310 (1988) 461; Nucl.Phys. B386 (1992) 215.
- [8] S.Catani and F.Hautmann. Phys.Lett. B315 (1993) 475; Nucl.Phys. B427 (1994) 475.
- [9] S.Camici and M.Ciafaloni. Nucl.Phys. B467 (1996) 25; Phys.Lett. B396 (1997) 406.
- [10] P.Hägler et al. Phys.Rev. D62 (2000) 71502.
- [11] L.V.Gribov, E.M.Levin and M.G.Ryskin. Phys.Rep. 100 (1983) 1.
- [12] E.M.Levin and M.G.Ryskin. Phys.Rep. 189 (1990) 267.
- [13] E.M.Levin, M.G.Ryskin, Yu.M.Shabelski and A.G.Shuvaev. Sov.J.Nucl.Phys. 53 (1991) 657.
- [14] E.M.Levin, M.G.Ryskin, Yu.M.Shabelski and A.G.Shuvaev. Sov.J.Nucl.Phys. 54 (1991) 867.
- [15] M.G.Ryskin, Yu.M.Shabelski and A.G.Shuvaev. Z.Phys. C69 (1996) 269.
- [16] V.A.Saleev and N.P.Zotov. Mod.Phys.Lett. A11 (1996) 25.
- [17] Yu.M.Shabelski and A.G.Shuvaev. Eur.Phys.J. C6 (1999) 313.
- [18] S.P.Baranov and M.Smizanská. Phys.Rev. D62 (2000) 014012.

- [19] S.P.Baranov and N.P.Zotov. hep/ph-0103138
- [20] M.G.Ryskin, Yu.M.Shabelski and A.G.Shuvaev. Yad.Fiz. 64 (2001) 123; hep-ph/9907507.
- [21] M.G.Ryskin, Yu.M.Shabelski and A.G.Shuvaev. Yad.Fiz. 64 (2001) 2080; hep-ph/0007238.
- [22] M.G.Ryskin, Yu.M.Shabelski and A.G.Shuvaev. hep-ph/0011111.
- [23] J.C.Collins, D.E.Soper and G.Sterman. Nucl.Phys. B308 (1988) 833.
- [24] S.J.Brodsky, G.P.Lepage and P.B.Mackenzie. Phys.Rev. D28 (1983) 228.
- [25] S.Narison. Phys.Lett. B341 (1994) 73; hep-ph/9503234.
- [26] P.Ball, M.Beneke and V.M.Braun. Phys.Rev. D52 (1995) 3929.
- [27] M.N.Mangano, P.Nason and G.Ridolfi. Nucl. Phys. B405 (1993) 507.
- [28] J.Blumlein. Preprint DESY 95-121 (1995).
- [29] E.A.Kuraev, L.N.Lipatov and V.S.Fadin. Sov.Phys.JETP 45 (1977) 199.
- [30] Yu.L.Dokshitzer, D.I.Dyakonov and S.I.Troyan. Phys.Rep. 58 (1980) 270.
- [31] M.A.Kimber, A.D.Martin and M.G.Ryskin. Eur.Phys.J. C12 (2000) 655; hep-ph/9911379.
- [32] M.Ciafaloni. Nucl.Phys. B296 (1988) 49.
- [33] S.Catani, F.Fiorane and M.Ciafaloni. Phys.Lett. B234 (1990) 339; Nucl.Phys. B336 (1990) 18.
- [34] G.Marchesini. In Proc. of the Workshop "QCD at 200 TeV", Erice, Italy (1990), ed. by L.Cifarelli and Yu.L.Dokshitzer, Plenum Press, New-York 1992, p.183.
- [35] M.A.Kimber, J.Kwiecinski, A.D.Martin, A.M.Stasto, Phys. Rev. D62 (2000) 094006.
- [36] Yu.M.Shabelski and A.G.Shuvaev. hep-ph/0107106
- [37] J.Kwiecinski, A.Martin and A.Stasto. Phys.Rev. D56 (1997) 3991.

- [38] M.Gluck, E.Reya and A.Vogt. Z.Phys. C67 (1995) 433.
- [39] M.Gluck, E.Reya and A.Vogt. Eur.Phys.J C5 (1998) 461.
- [40] G.P.Lepage. J.Comp.Phys. 27 (1978) 192.
- [41] D0 Coll., B.Abbott et al. Phys.Lett. B487 (2000) 264.
- [42] D0 Coll., B.Abbott et al. Phys.Rev.Lett. 84 (2000) 5068.
- [43] CDF Coll., D.Acosta et al. Phys.Rev. D66 (2002) 032002; hep-ex/0206019.
- [44] CDF Coll. D.Acosta et al. hep-ex/0307080.
- [45] A.V.Lipatov, L.Lönnblad, N.P.Zotov, hep-ph/0309207.
- [46] M.Cacciari et al. hep-ph/0312132.
- [47] ZEUS Coll., M.Derrick et al. Phys.Lett. B349 (1995) 225.
- [48] H1 Coll. Preprint DESY 96-055.
- [49] H1 Coll. Phys.Lett. B467 (1999) 156.
- [50] L.Apanasevich et al. Phys.Rev. D59 (1999) 074007.
- [51] A.K.Likhoded and S.R.Slabospitsky. Phys.Atom.Nucl. 60 (1997) 981; 62 (1999) 693; hep-ph/0008230.
- [52] J.Dias de Deus and F.Durães. Eur.Phys.J. C13 (2000) 647.
- [53] Yu.M.Shabelski. hep-ph/001103

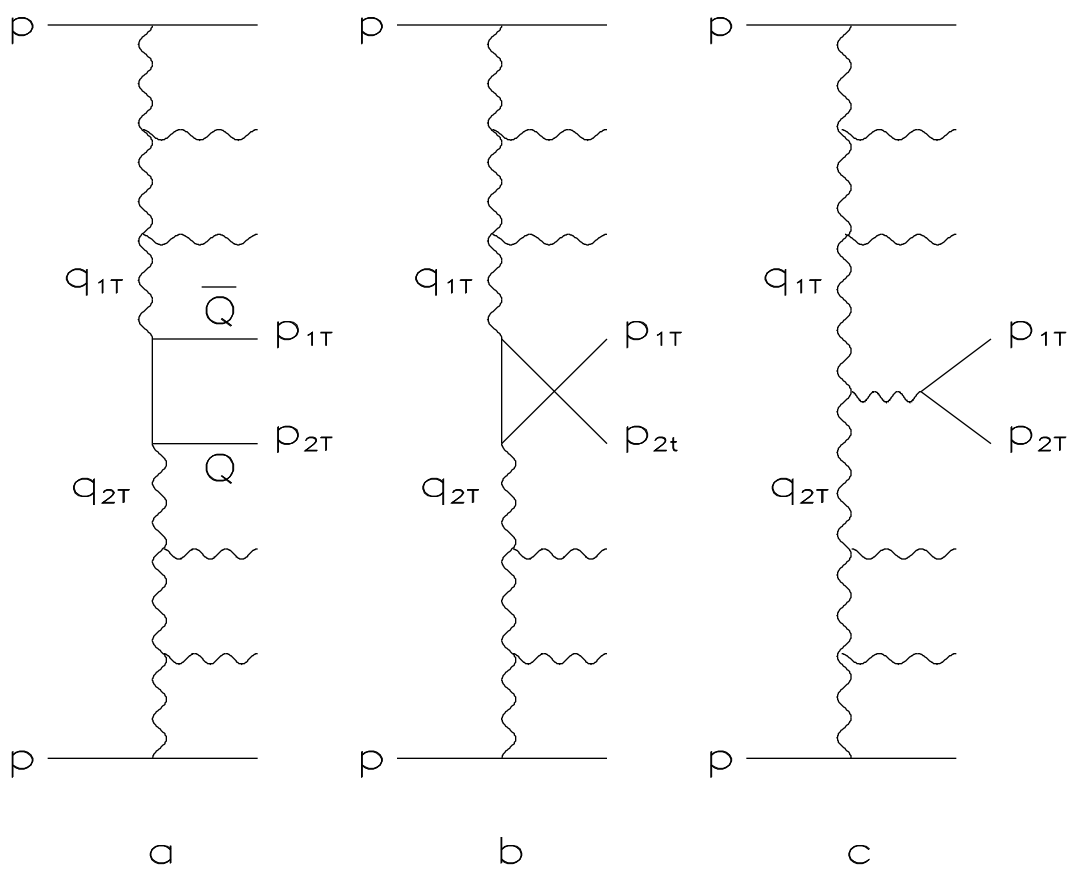


Fig. 1

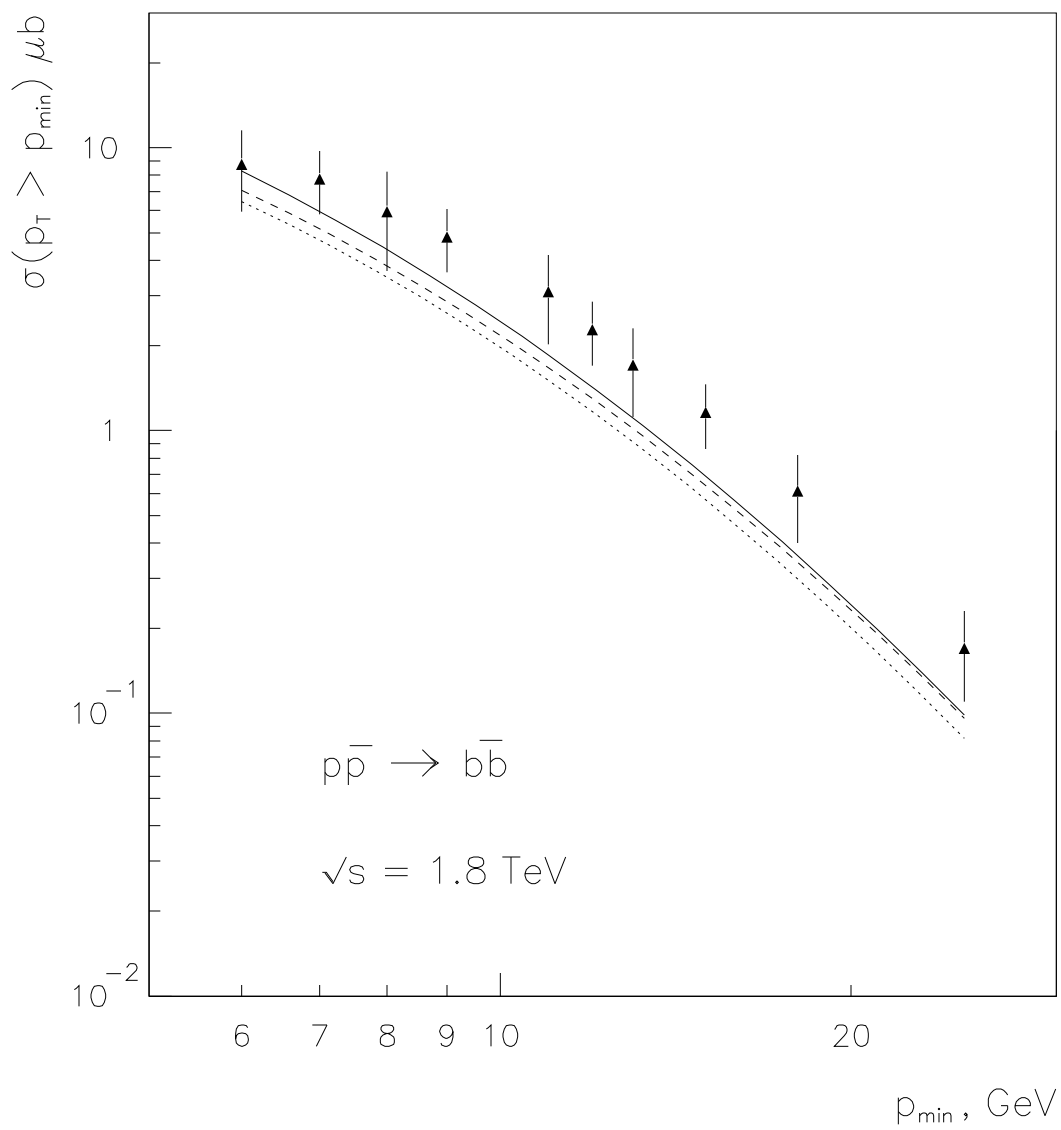


Fig. 4a

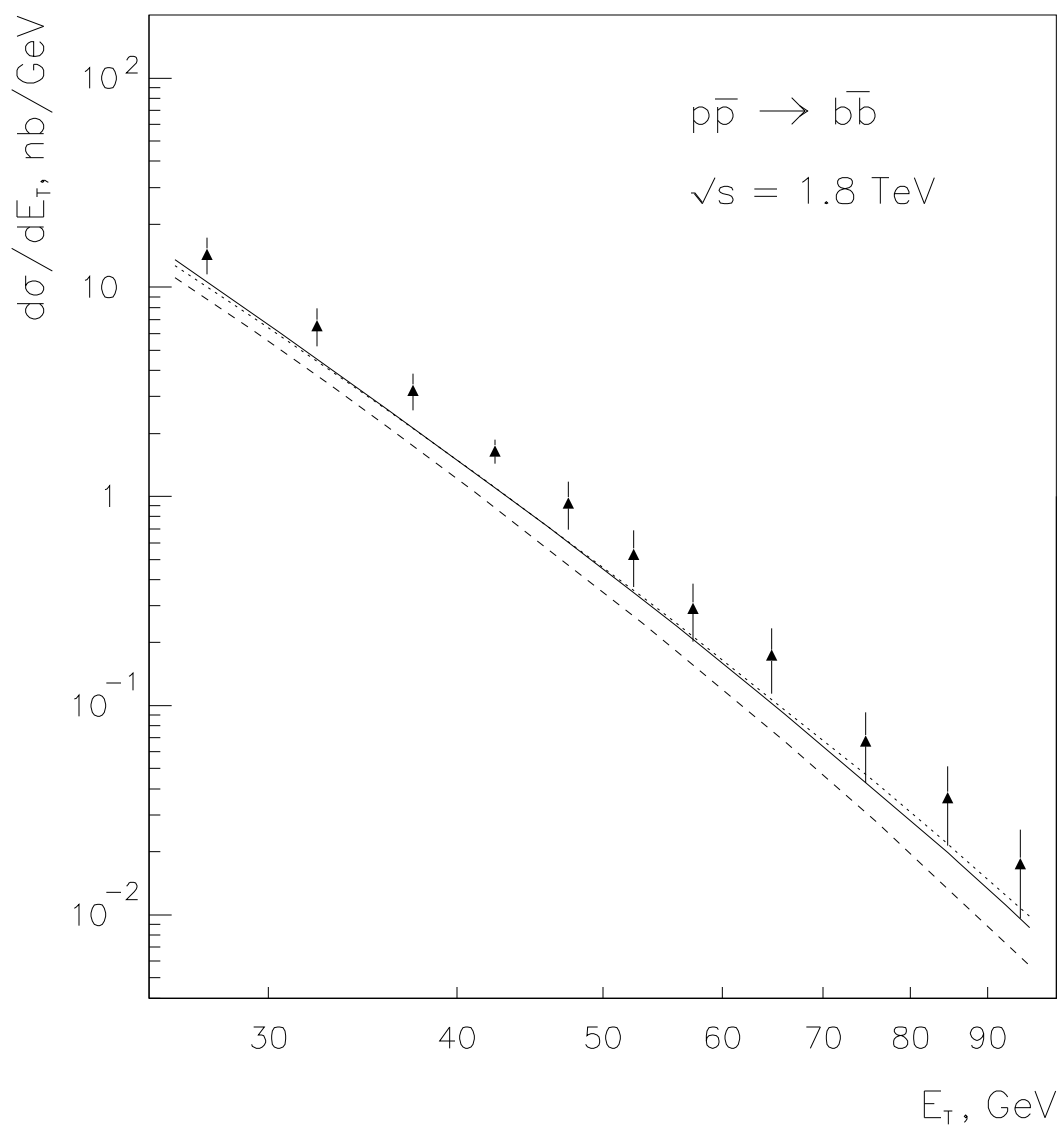


Fig. 4b

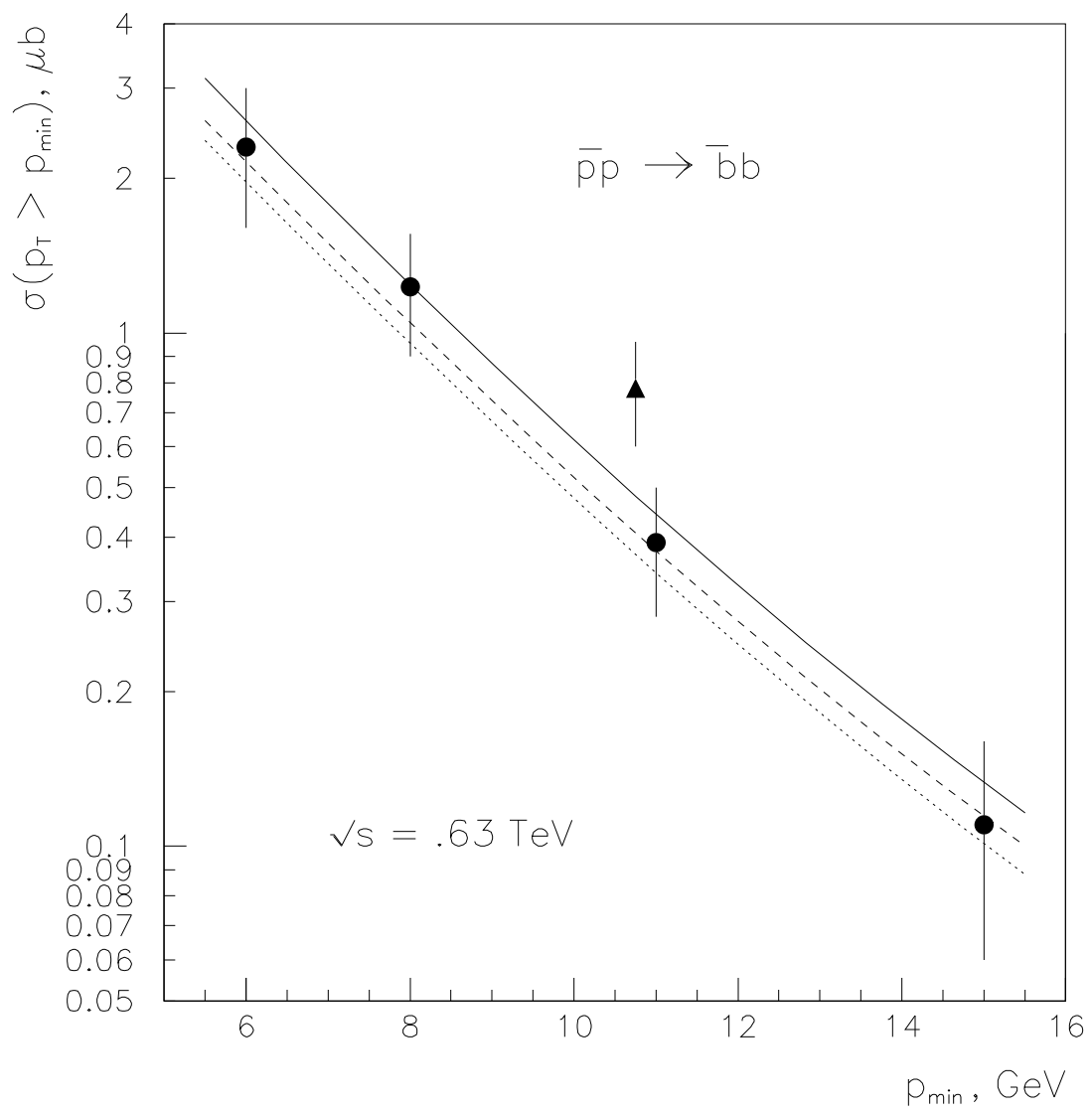


Fig. 4c

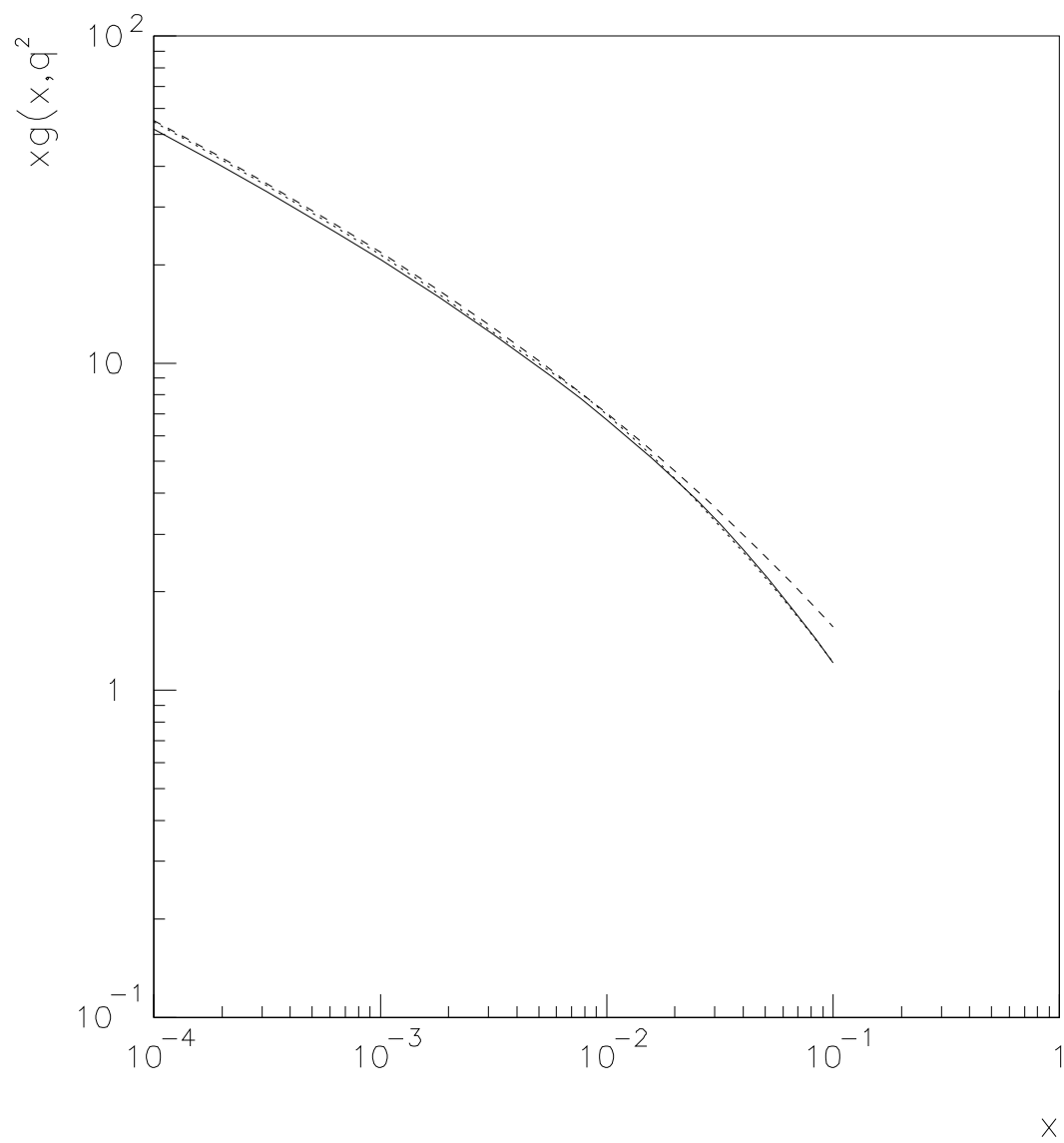


Fig. 3a

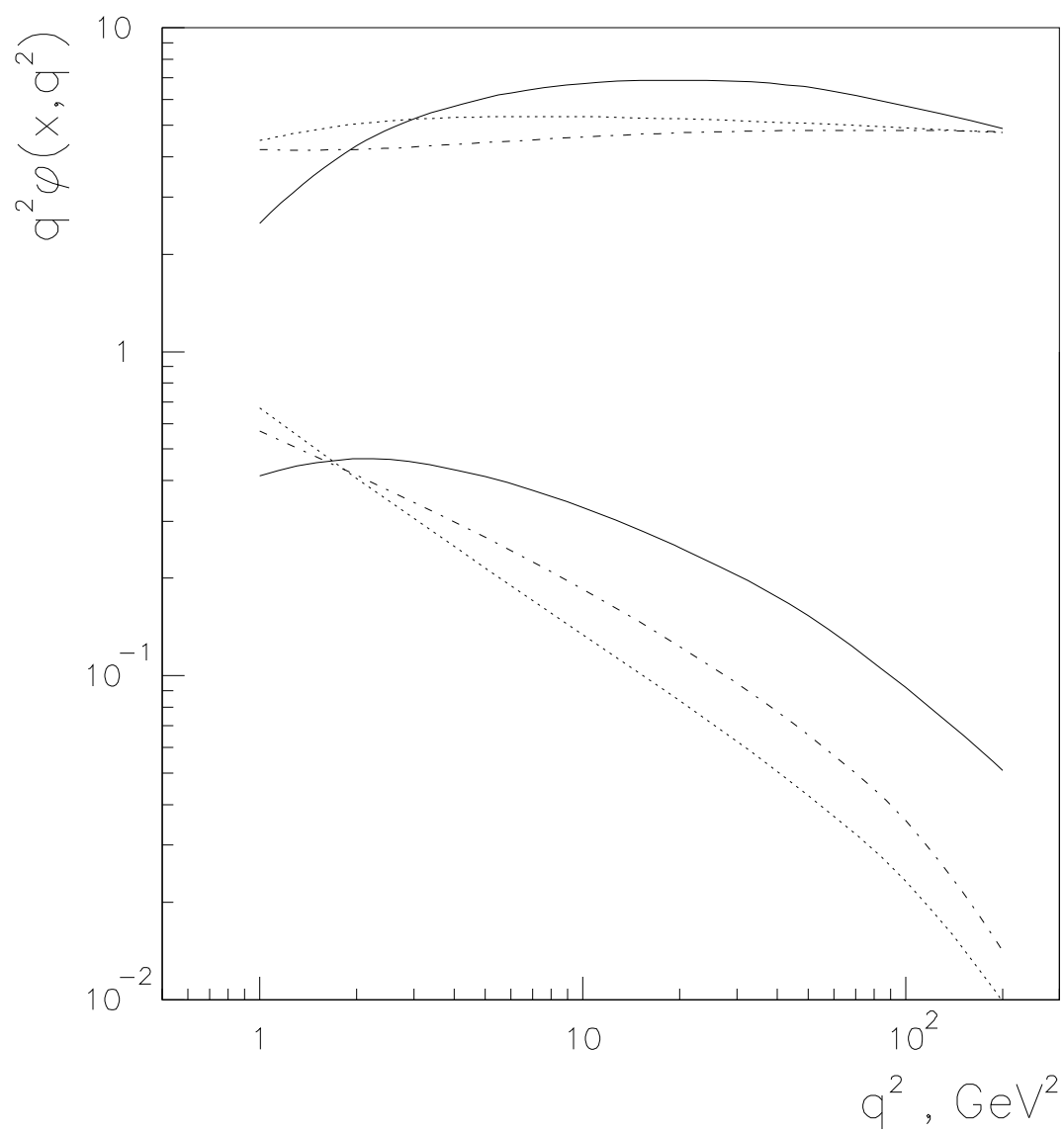


Fig. 3b

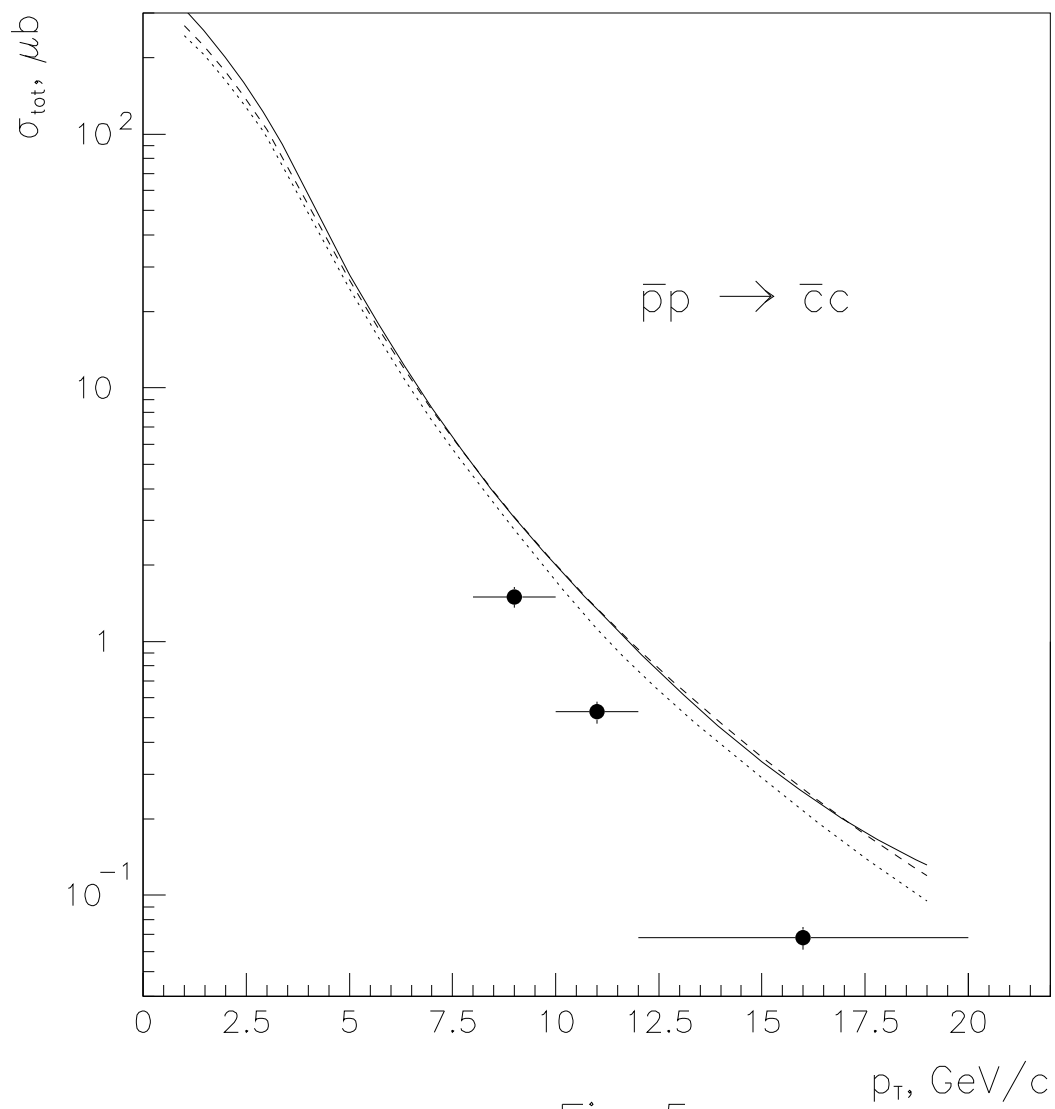


Fig. 5

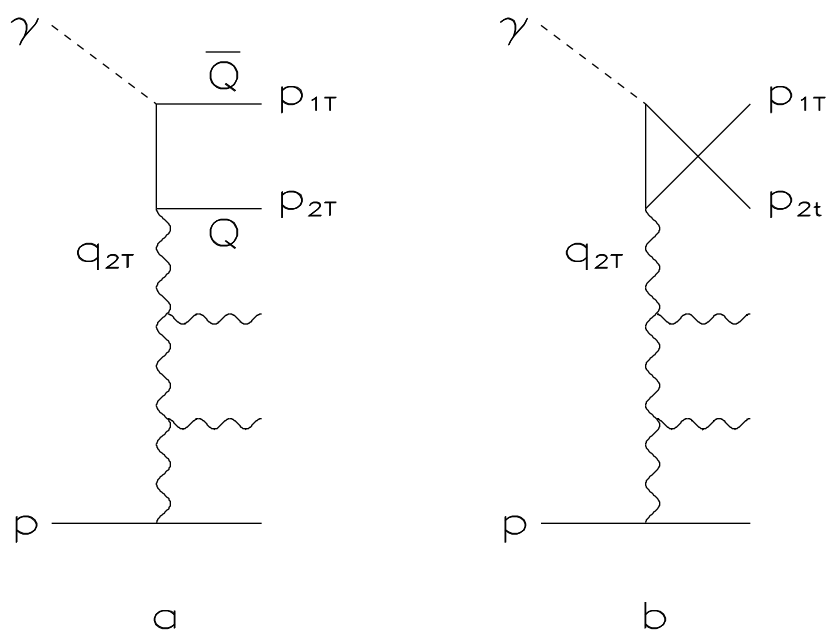


Fig. 2

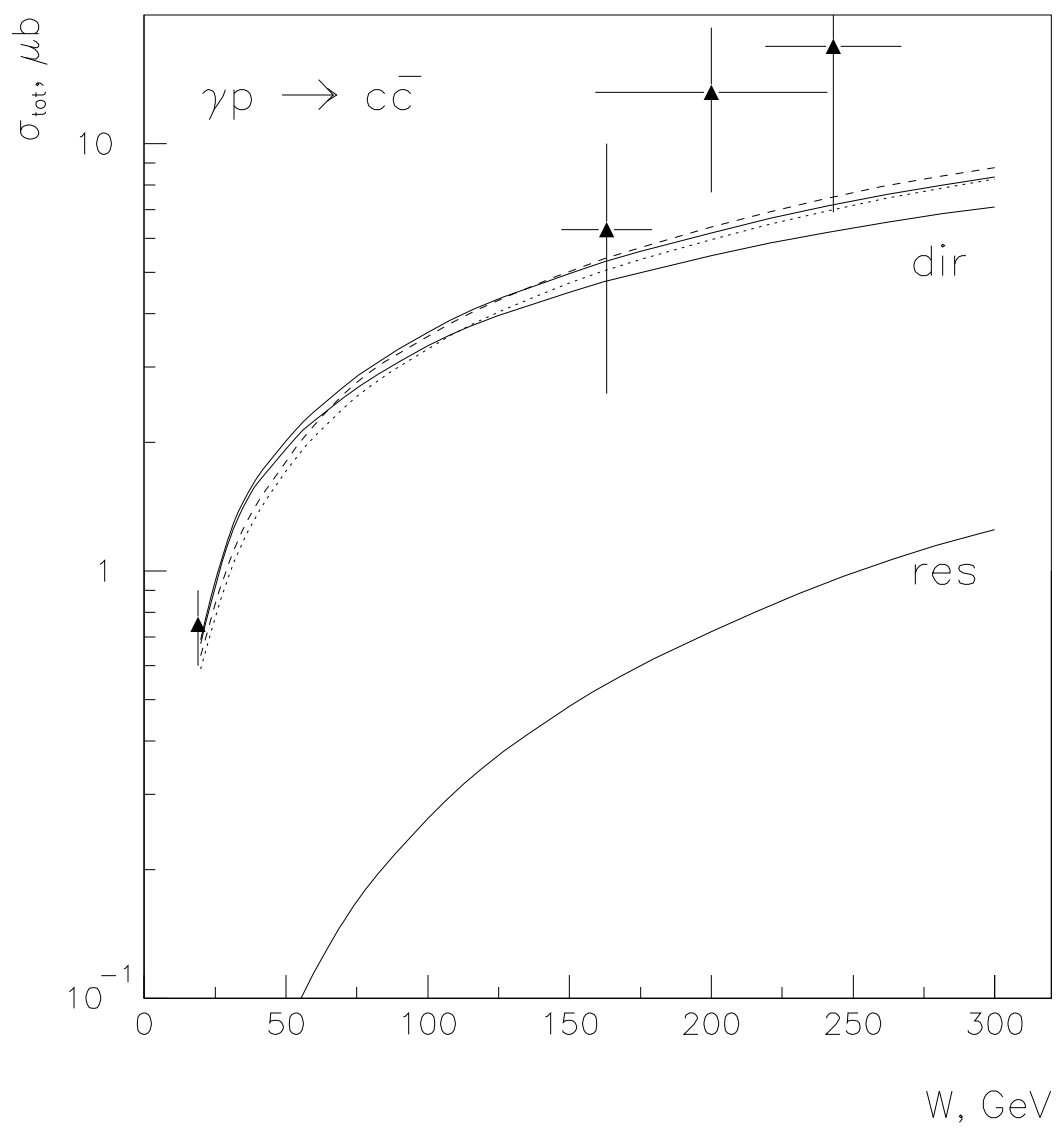


Fig. 6a

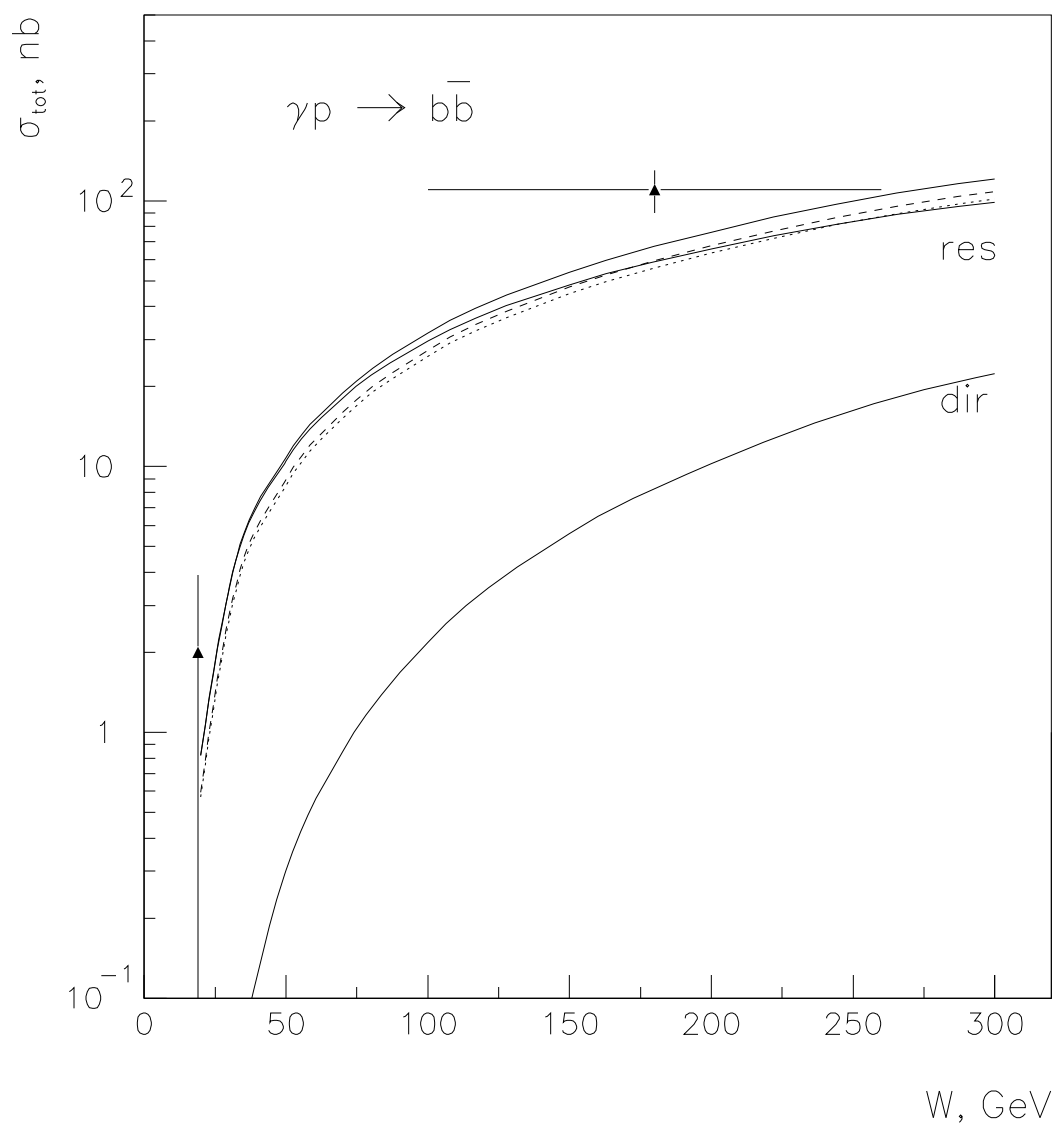


Fig. 6b